

ELEMENTARY STEPS IN SYNAPTIC TRANSMISSION REVEALED BY CURRENTS THROUGH SINGLE ION CHANNELS

Nobel Lecture, December 9, 1991

by

BERT SAKMANN

Max-Planck-Institut für medizinische Forschung, W-6900 Heidelberg,
Germany

INTRODUCTION

The plasma membrane of a cell separates its interior from the extracellular environment and from other cells and acts both as a diffusional barrier and as an electrical insulator. This allows differentiation of cells with specialized functions. Coordinated behaviour of multicellular organisms requires exchange of signals between individual cells. Because the signal must be transferred from one cell to another, it must occur by a mechanism that allows it to traverse the insulating cell membrane. Signalling occurs in various ways via specific receptors on the receiving cells and subsequent generation of a transmembrane signal. The nervous system connects cells in a very specific way and signal transmission between individual cells takes place at contacts, called synapses, that are anatomically and functionally highly specialized for rapid communication.

Synaptic signal transmission is used preferentially for rapid communication between cells of the nervous system and those cells of peripheral organs which are responsible for sensory transduction as well as for the generation of secretory and motor activity (Katz, 1966; 1969). Synaptic transmission includes a chemical step, where the signalling substance, called a transmitter, is released very locally from the sending, presynaptic cell and then acts transiently on receptors of the receiving, postsynaptic cell. The receptor is part of an ion channel and mediates, upon occupation by the transmitter, a brief flux of ions across the postsynaptic membrane generating a change in the postsynaptic membrane potential.

The signal that actually initiates the cellular response of the postsynaptic cell is the flux of ions across the postsynaptic membrane. The size, duration and direction of this ion flux, as well as the nature of the ions traversing the postsynaptic membrane, determines whether this response will either activate voltage sensitive membrane conductances and initiate action potentials, or instead reduce the cells electrical activity. The cellular response may also be determined by a change in intracellular ion concentrations, in

particular the concentration of calcium ions, which act as a second messenger for many cellular responses like contraction or secretion.

The neuromuscular junction is often thought of as a prototypical synapse. At the neuromuscular junction the nerve terminal of a motoneurone releases acetylcholine (ACh) and generates end-plate potentials (EPPs), which in turn activate voltage sensitive conductances to transmit excitation into other parts of the muscle fibre (Katz, 1966). The current flow across the end-plate, induced by the release of packets of ACh, results from the superposition of many small individual 'elementary' events (Katz and Miledi, 1972) and there is ample evidence that postsynaptic potentials in other synapses are also generated by the superposition of elementary events.

This lecture describes the properties of elementary currents underlying postsynaptic potentials as well as their molecular determinants. The focus is primarily on the properties of elementary currents mediating neuromuscular transmission. The neuromuscular junction is the synapse characterized best, both functionally and in its molecular constituents, and most of the techniques for recording single channel currents were developed with the muscle fibre preparation. It has turned out that, apart from important details, a comparable behaviour of elementary currents is observed for other transmitter activated postsynaptic potentials, particularly those 'activated by glycine, γ -aminobutyric acid (GABA), glutamate and serotonin. These transmitters mediate 'rapid' synaptic transmission in the central nervous system (CNS) and produce postsynaptic potentials lasting milliseconds to hundreds of milliseconds.

ELEMENTARY EVENTS

End-plate current noise: The notion of 'elementary events' was introduced by B. Katz and R. Miledi when they observed 'membrane noise' during recording of membrane depolarisations induced by ACh applied from a iontophoretic pipette to end-plates of frog skeletal muscle (Katz and Miledi, 1972). They suggested that the increase in noise associated with depolarisation is the result of the independent superposition of elementary events generated by random activation of individual acetylcholine receptors (AChRs), each activation causing a minute depolarisation.

The estimates of the size of the conductance change generating an elementary event derived from such noise measurements, assuming a pulse shaped conductance change, were of the order of 30 to 50 Picosiemens (pS) and had a duration of only a few milliseconds (Katz and Miledi, 1972; Anderson and Stevens, 1973). This means that the amplitude of an elementary current would be on the order of 3 – 5 Picoamperes (pA). This size is about two to three orders of magnitude smaller than what could be resolved by the intracellular recording techniques available at the time (Neher, 1991).

Current noise in extrasynaptic muscle membrane: ACh sensitivity is restricted, in normal muscle fibres, to a very small area of the muscle which is located

underneath the nerve terminal. Following chronic denervation of skeletal muscle, effected by severing the motor nerve, the entire muscle becomes ACh supersensitive (Axelson and Thesleff, 1959). It is now known that this is due to the incorporation of newly synthesized ACh receptors into the extrasynaptic surface membrane of muscle fibres. Using noise analysis of ACh-activated currents we estimated the average conductance increase underlying elementary events in denervated frog muscle fibres to be about 20 pS (Neher and Sakmann, 1976a). The size of the elementary current in denervated fibres was thus smaller (about 60% of normal). The average duration of the elementary event was however 3 to 5 times longer than that of elementary events in the end-plate.

ELEMENTARY END-PLATE CURRENTS ARE PULSE SHAPED

Solving the background noise problem: Denervated, supersensitive frog muscle fibres were thus the preparation of choice for developing methods for recording from single channels and to investigate the basic properties of ion channels by direct measurement of elementary events. The key for the reduction of the background noise in the relevant frequency range (up to 1 kHz) was to restrict the measurement to a small membrane area of about 10 μm^2 and to isolate this membrane patch electrically from the rest of the cell membrane by sealing the narrow tip of the glass pipette tightly onto the membrane (Neher, 1991). Pressing the pipette against a normal muscle fibre resulted in seal resistances of less than 1 M Ω and often damaged the fibre. The sealing problem was solved by exposing the fibre to mild enzymatic treatment which freed muscle fibres from their covering connective tissue and the basement membrane and thus exposing the bare sarcolemma (Betz and Sakmann, 1973) and by polishing the tip of the pipette with a small heating filament (Neher, Sakmann and Steinbach, 1978). When the polished tip of the patch pipette was pressed gently against the bare sarcolemmal membrane of single fibres, secured mechanically by a glass hook, seal resistances of 50 to 150 M Ω were obtained. The membrane potential of the fibre was set locally, close to the membrane patch from which the patch current was recorded, by a conventional voltage clamp amplifier with two intracellular microelectrodes (Fig. 1A).

Single channel currents: Using these precautions to obtain adequately high seal resistances (> 50 M Ω) and using suberyldicholine, an agonist causing ACh receptors to open for longer periods, we were able to record current blips from denervated frog muscle fibres which were pulse shaped, and which had many of the hallmarks of the elementary events that had been inferred from noise analysis of ACh-activated currents (Neher and Sakmann, 1976b). Square-pulse shaped currents were also recorded from denervated rat muscle. They were similar to those obtained from denervated frog muscle, and in both preparations the directly measured amplitudes of elementary events agreed reasonably well with the estimated size derived

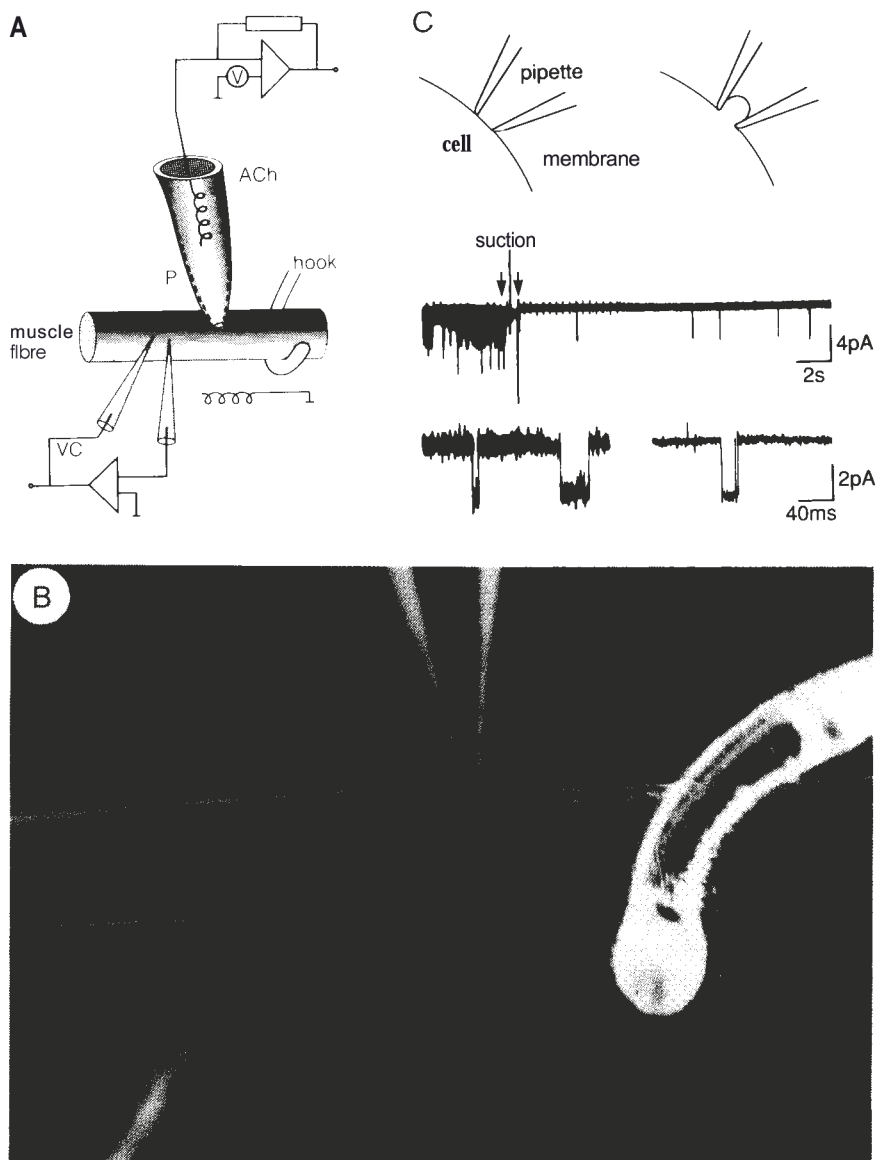


Figure 1. Recording from a patch of end-plate membrane. A: Schematic diagram of muscle fibre with tip of patch pipette sealed against the cleaned surface of a single muscle fibre. The pipette is filled with extracellular solution and the pipette potential is held isopotential with the extracellular solution by means of feedback circuit. The fibres membrane potential is clamped to a command value by a two microelectrode voltage clamp amplifier and two intracellular microelectrodes. Patch pipette contains in addition low concentration of acetylcholine (ACh). B: Disjunction of nerve terminal from muscle fibre. Photomicrograph of a single frog muscle fibre with bare end-plate after removal of the nerve terminal. The tip of the patch pipette is touching the end-plate (light streak). Two intracellular microelectrodes are used to locally clamp the membrane potential of the fibre. A glass hook seen on the right side secures the fibre mechanically. Calibration bar is 50 μm . C: Single channel current recording with seal resistances in the $\text{M}\Omega$ and $\text{G}\Omega$ range, respectively. Schematic drawing on top shows the formation of a high resistance seal by application of negative pressure ('suction') to pipette interior. Traces represent records, at two time scales, of elementary end-plate currents from the same membrane patch before (left) and after (right) application of negative pressure to the pipette interior ('suction') which increased the seal resistance of the pipette-membrane contact from 150 $\text{M}\Omega$ to 60 $\text{G}\Omega$ (from Hamill et al., 1981).

from fluctuation analysis of ensemble voltage clamp currents (Sakmann, 1978).

Disjunction of the neuromuscular synapse: To relate the properties of elementary currents to synaptic transmission at the end-plate of *normal* muscle fibres, it was necessary to compare the properties of elementary events with those of miniature end-plate currents (MEPCs). To place the tip of the patch pipette onto the end-plate, the neuromuscular junction must be visible and the nerve terminal, which covers the end-plate in normal fibres, must be removed from the end-plate. This is most easily accomplished by localized application of collagenase, followed by a gentle stream of Ringer's solution delivered from a pipette with a small (100 pm) tip opening. This procedure resulted in single muscle fibre preparations with their end-plates freely accessible (Fig. 1 B).

Elementary end-plate currents: The elementary events recorded from the end-plate membrane (elementary end-plate current) were about 50% larger in amplitude, but considerably shorter in duration than those measured in the extrasynaptic membrane, as expected from the fluctuation analysis of ACh activated currents in normal and denervated fibres (Neher and Sakmann, 1976a). The measurements demonstrated that the elementary end-plate current is a square pulse-like event allowing passage of small cations like Na^+ , K^+ or Cs^+ at a very high rate (10^7 – 10^8 s^{-1} , thus suggesting that these currents reflect the opening of an aqueous pore across the membrane (Neher and Sakmann, 1976b).

Some basic properties of end-plate channels became apparent only at the improved resolution that resulted from the reduction of background noise by establishment of pipette - membrane seals with resistances in the range of several $\text{G}\Omega$ (Hamill et al., 1981). Using freshly pulled pipettes and applying slight negative pressure to the pipette interior, thereby pulling the patch of membrane underneath the tip opening into the pipette tip, a molecular contact between the glass and the plasma membrane was established which improved the seal resistance from 50 – 150 $\text{M}\Omega$ to the range of 1 – 100 $\text{G}\Omega$. Consequently, the amplitude of the background noise was reduced and rim currents (Neher et al., 1978) were almost absent (Fig. 1C). The reduced background noise allowed us to perform recordings of elementary end-plate currents with up to 10 kHz bandwidth and to examine quantitatively the fine details of elementary end-plate currents that became apparent at this resolution.

Unitary conductance of the open end-plate channel: Records of elementary end-plate currents (Fig. 2A) indicated that the end-plate channel exists in only two conductance states: either the channel is closed, when there is no agonist occupying the binding site(s) or it is fully open when the binding site(s) are occupied. The amplitude distribution of a large number of elementary end-plate currents is fitted by a single Gaussian curve (Fig. 2B) where the variance in the amplitude distribution is mostly due to the remaining background noise of the recording. This confirmed the initial inference that end-plate channels prefer two conductance states, fully closed and fully open (schematic diagram, Fig. 2A).

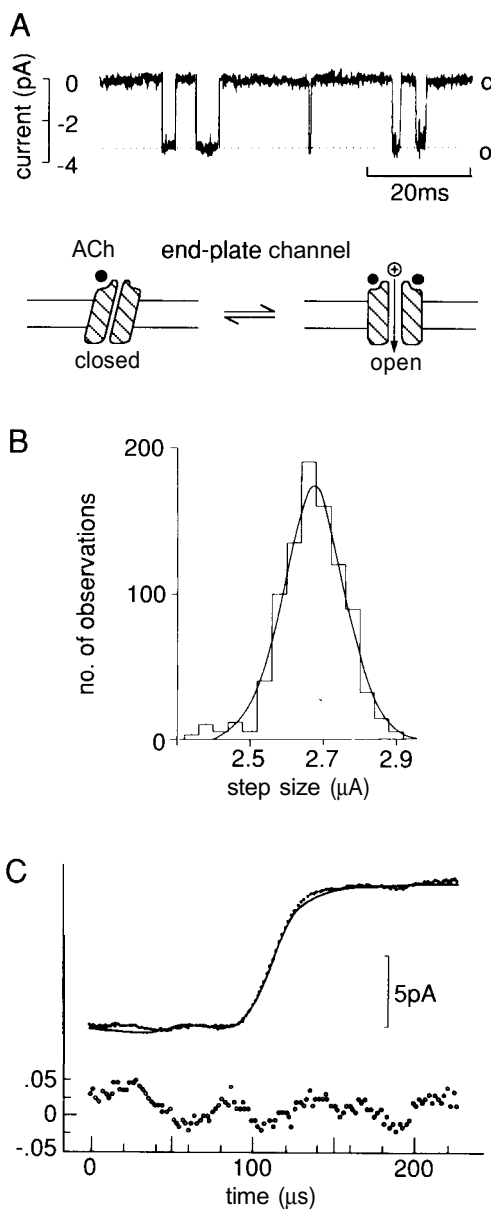


Figure 2. Elementary end-plate currents. A: Trace of elementary end-plate currents from rat muscle activated by acetylcholine (ACh). Membrane potential was -70 mV. The schematic drawing under the current trace illustrates the opening and closing of an end-plate channel by transmitter binding and unbinding to recognition site on the end-plate channel. The channel is closed in the resting state and is open when two agonist binding sites are occupied by ACh molecules. B: Distribution of elementary end-plate current amplitudes, activated by 200 nM ACh in frog muscle. Histogram is fitted by a Gaussian curve with mean of 2.69 ± 0.10 pA. C: End-plate channels open rapidly to a unitary conductance. Upper traces show superposition of leading edges of elementary end-plate current (points) and of record of step-test pulse (continuous line, after amplitude scaling) to measure the frequency response of the recording system. Relative difference between the two aligned records is shown below (open circles).

Time course of channel closed-open transitions: The time course of the single channel current reports structural transitions of a single macromolecule in real time. An obvious question therefore is whether the time course of the transition between the open and closed channel states is measurable (Fig. 2C). We superimposed the time course of the leading or trailing edge of a single channel current on that of the step response of the recording system. Since no difference was detected the rise time course of single channel currents must have been limited by the frequency response of the recording system. The time constant of the channel transition from the closed to the open states thus is less than 10 ps.

Observing the same channel repeatedly: To resolve elementary end-plate currents the concentration of ACh or a related agonist like suberyldicholine in the pipette, was low (usually below 0.5 μM) to ensure that the opening of end-plate channels was infrequent and individual openings were clearly separated from each other (Fig. 2A). This implied however that one could not be sure that successive elementary end-plate currents reflect the opening of the same individual end-plate channel, since it is likely that several channels are present in the membrane patch under investigation. In the presence of higher agonist concentrations (for acetylcholine > 5 μM) we found that elementary currents appear in long bursts of several hundreds of milliseconds duration. The reason for the occurrence of current bursts is that the channel can adopt, in addition to the 'resting closed' state, an additional, kinetically distinct, closed state designated as 'desensitized closed' state. This state is almost absorbing and channels isomerize only occasionally back to the open or 'resting closed' states. When this happens the same channel switches back and forth between its 'resting closed' and the 'open' state repeatedly before it enters again the desensitized closed state (Sakmann et al., 1980) thus allowing the observation of several openings and closures of the same individual channel. The fact that the amplitude of the elementary currents during such an epoch did not change and that the average durations of end-plate current were essentially independent of ACh concentration supported the two-state reaction scheme to explain the current recordings shown in Fig. 2A.

ELEMENTARY STEPS IN NEUROMUSCULAR TRANSMISSION

Miniature end-plate currents and elementary end-plate currents: An obvious question related to the function of the end-plate channel in synaptic transmission is that of the relation between the size and duration of the elementary end-plate currents and that of the synaptic currents. In other words, how is the time course of the end-plate currents related to the gating properties of the end-plate channel?

A simple way to reconstruct the decay of a miniature end-plate current (MEPC), the signal transmitted across the neuromuscular junction following the release of a single vesicle of transmitter, is to align several hundreds or thousands of elementary end-plate currents at their leading edge and

superimpose them. The hypothesis behind this procedure is that, following the release from a presynaptic vesicle, the concentration of ACh in the synaptic cleft rises very rapidly (in less than 1 ms) to saturate ACh receptors, and then rapidly decays again to negligible values (Magleby and Stevens, 1972). If the ACh concentration transient in the cleft is very brief in comparison to the average duration of elementary end-plate currents then the decay of MEPCs would reflect the distribution of the durations of elementary end-plate currents after removal of ACh. In Fig. 3 individual

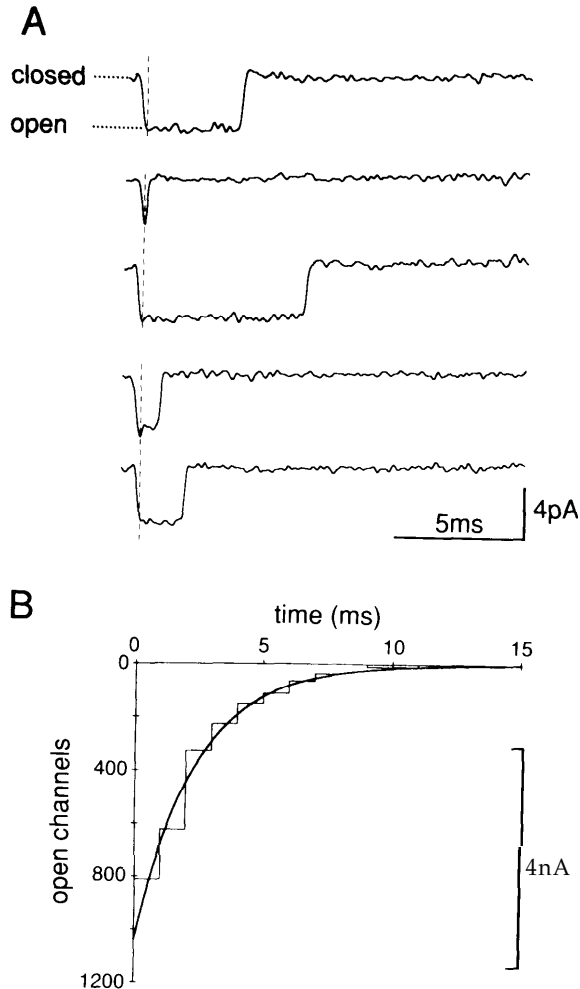


Figure 3. Elementary end-plate current duration determine shape of miniature end-plate currents. A: Records of elementary end-plate currents activated by 200 nM ACh in rat muscle fibre aligned at their leading edges to illustrate variation in duration of elementary end-plate currents. B: Average of 1000 superimposed elementary end-plate currents. Individual elementary end-plate current were digitized by time course fitting (Colquhoun and Sakmann, 1985) and superimposed on the histogram represents single exponential with decay time constant of 2.7 ms.

elementary end-plate currents are aligned at their leading edges (Fig. 3A). The current generated by superposition of 1000 elementary end-plate currents has a peak of 4.7 nA and decays with a time constant of 2.7 ms (Fig. 3B). These values are similar to those of MEPCs recorded from rat muscle end-plates. This suggests that a single MEPC, which reflects a quantal conductance increase of approximately 50 nS, is generated by the almost simultaneous opening of about one thousand end-plate channels (each with 50 pS conductance), and that the decay of MEPCs is determined to a first approximation, by the average duration of the elementary end-plate currents.

Elementary currents reflect bursts of single channel openings: The time course of elementary end-plate currents is more complicated in shape than expected from a channel that switches between an open and a single closed state as assumed in Fig. 2A. Most elementary end-plate currents, when examined at high time resolution, are interrupted by very short gaps (Fig. 4A, B), i. e. the current returns transiently to the base line (Colquhoun and Sakmann, 1981; Colquhoun and Sakmann, 1985). This behaviour is observed in almost all transmitter- and voltage-gated ion channels investigated so far. In the case of the end-plate channel, it reflects the fact that, when the receptor has bound ACh, the channel opens and closes several times before the agonist dissociates from the receptor. The scheme shown in Fig. 2A is intended only to illustrate the basic principle of structural transitions of the channel and assumes only one open and one closed channel state. In reality, however, a reaction scheme consistent with the experimental observations involves several closed and open states. The observed behaviour of the current during a single elementary event is in fact predicted by a reaction involving transition of the closed, resting receptor to the open state via an intermediate closed state (Colquhoun and Hawkes, 1977).

Plausible reaction scheme for end-plate channel activation: We investigated the fine structure of these brief transitions for end-plate channels in collaboration with D. Colquhoun. Using the tools of probability theory (Colquhoun and Hawkes, 1982), it was possible to derive the minimum number of states the channel can adopt and also the rates of transition from one state to another (Colquhoun and Sakmann, 1985). At least five kinetically distinct states (Fig. 4C) could be discriminated from the measurement of both the open and closed time distributions at low concentrations of several agonists, and the derived reaction rates satisfactorily described the time interval distributions. It represents a scheme for the gating of the end-plate channel by ACh during normal neuromuscular transmission and is a modification of the scheme proposed initially by Del Castillo and Katz (1957). It comprises a resting, unliganded state and four liganded states two of which are open states. The derived microscopic rate constants (Fig. 4D), which describe the transitions between the various states of the end-plate channel, indicate that the open probability of the channel at high the ACh concentrations occurring during neuromuscular transmission (higher than 100 μ M) is close to unity. This implies that ACh acts on the end-plate channel as a transmitter

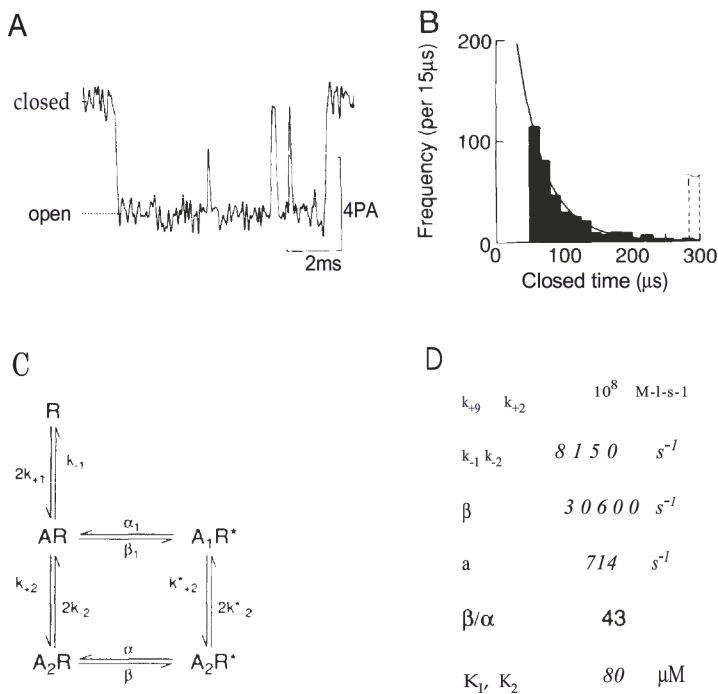


Figure 4. Reaction scheme for end-plate channel activation by ACh as derived from burst analysis of elementary end-plate currents. **A:** Record of elementary end-plate current activated by suberyldicholine, an agonist of acetylcholine, to illustrate burstlike appearance of elementary end-plate currents. Note unresolved brief closure. **B:** Distribution of durations of brief closures measured during elementary end-plate currents. Continuous line represents exponential with decay time constant of 39 μs. **C:** Reaction scheme for interaction of ACh (A) and end-plate channel (R) comprising five, kinetically distinct, states. Conducting states are marked by asterisk. **D:** Derived rate constants for interaction of ACh and end-plate channel for the reaction scheme shown in C. k_+ and k_- are microscopic dissociation constants at the two binding sites for ACh (from Colquhoun and Sakmann, 1985).

with high efficacy. When an ACh receptor is doubly liganded the equilibrium between the open and the closed states is shifted almost completely to the open state indicating that the end-plate channel is very effective in rapidly passing current through the end-plate.

ISOFORMS OF ENDPLATE CHANNELS

When recording postsynaptic currents in muscle fibres from young animals we found, in collaboration with H. Brenner, that there is a marked change in the decay time course of MEPCs during postnatal development. This reflects a switch of the functional properties of end-plate channels during this time. Up to postnatal day 8 (P8), the decay of the MEPCs is slower than that of MEPC recorded in the adult muscle. During the period of P7 to P15, the MEPC decays are described best by the sum of two exponentials whereas after P21 that time the fast decay observed in adult fibres, pre-

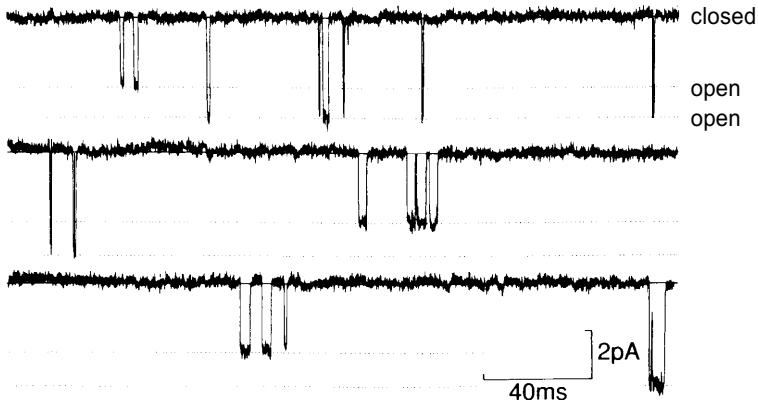


Figure 5. Two classes of elementary end-plate currents. Record of single channel currents activated by $0.5 \mu\text{M}$ ACh in postnatal (P8) rat muscle fibre. Two classes of elementary currents, with different amplitudes and average durations, are observed in this patch. The elementary currents with the larger amplitude correspond to end-plate currents observed in adult fibres ($> \text{P21}$), whereas elementary currents of smaller amplitude correspond to those seen predominantly at early postnatal stages ($< \text{P8}$) or in fetal muscle.

dominates (Sakmann and Brenner, 1978; Michler and Sakmann, 1980). The molecular basis for this difference in synaptic currents is shown in Fig. 5. Two classes of elementary currents are recorded from muscle fibres at early postnatal stages. Mammalian skeletal muscle expresses two isoforms of end-plate channels which mediate different elementary end-plate currents (Hamill and Sakmann, 1981), differing both in amplitude and average duration. The expression of these channel isoforms is developmentally regulated. At early stages of development, in the uninnervated muscle, a fetal type of channel with lower conductance and longer average durations of elementary currents predominates. Following innervation the fetal isoform is replaced by the mature adult isoform which has a higher conductance and a shorter duration of elementary currents. Following denervation the fetal isoform is expressed again, suggesting that skeletal muscle expresses a mosaic of AChR channel isoforms and that the composition of this mixture of channel isoforms is under neuronal control (Sakmann et al., 1992 for review).

MOLECULAR DETERMINANTS OF CHANNEL FUNCTION

Identification of some of the molecular determinants of AChR channel function was achieved using patch clamp techniques and the tools of molecular biology. Biochemical work on *Torpedo* electroplax had shown that the AChR channel is assembled in a pseudosymmetric fashion from several subunits where each subunit contributes to the formation of the channel (Karlin, 1991; for review). In addition, it had been demonstrated that recombinant AChR channels can be reconstituted in a functional form in a host membrane by injecting the RNAs, that encode constituent subunits,

into the cytoplasm of *Xenopus laevis* oocytes (Miledi et al., 1989, for review). Following the isolation of the genes encoding the subunits of *Torpedo* electroplax and skeletal muscle AChRs, *in vitro* synthesized RNAs could be used to direct the synthesis of wild type and mutagenized recombinant AChR channels (Numa, 1989, for review). Whole-cell current measurements from oocytes, expressing recombinant AChR channels, though important in showing that only certain subunit combinations would assemble to functional AChR channels, lacked the detail necessary to demonstrate the similarity of recombinant and native AChRs or to draw conclusions on more specific structure-function relations. To relate functional properties of native AChRs to structural data single channel conductance measurements on recombinant AChRs were required.

Because the oocyte plasma membrane is ensheathed by a vitelline membrane the access of patch pipette tips to the plasma membrane is prevented. The vitelline layer may be removed and the bare oocyte membrane expressed without damaging it, by brief exposure of the oocyte to a strongly hypertonic potassium solution. Oocytes then shrink away from the covering vitelline layer, which can be mechanically removed, leaving the bare plasma membrane (Methfessel et al., 1986). This procedure enabled us to combine single channel conductance measurements with recombinant DNA techniques to identify structural determinants of AChR channel function. Two problems which are closely interrelated, the elucidation of the molecular basis of end-plate channel isoforms and the identification of structural determinants of the channels inner wall, were resolved in collaboration with a group of molecular biologists from the laboratory of S. Numa and with V. Witzemann.

Recombinant AChR channel subtypes: The molecular distinction between the two isoforms of the end-plate channel (Fig. 5) was clarified as a result of experiments where the cRNAs of the five muscle subunits were injected into oocytes, resulting in the functional expression of two AChR isoforms. Following the injection of cRNAs encoding the α -, β -, γ - and δ - or alternatively the α -, β -, δ - and ϵ -subunits two functionally different recombinant channel isoforms were generated (Fig. 6A, B). In their functional properties the two recombinant AChR isoforms resembled closely the two native AChR isoforms observed in muscle membrane (Mishina et al., 1986). Both the amplitude of single channel currents recorded from oocytes and their average duration (Fig. 6C) were similar to elementary currents observed in bovine or rat skeletal muscle (Mishina et al., 1986; Witzemann et al., 1987; Witzemann et al., 1990). Thus, it seems that native channel isoforms reflect differences in subunit composition of the channel, in the case of AChR channel an exchange between the γ - and ϵ -subunit is the molecular difference between the two channel subtypes (Fig. 6D, E).

Differential regulation of γ - and ϵ -subunit genes: The molecular mechanism underlying the switch in end-plate channel properties effected by the exchange of constituting subunits is a postnatal switch in the expression of the genes encoding the γ - and ϵ -subunit. Northern blot analysis of total RNAs

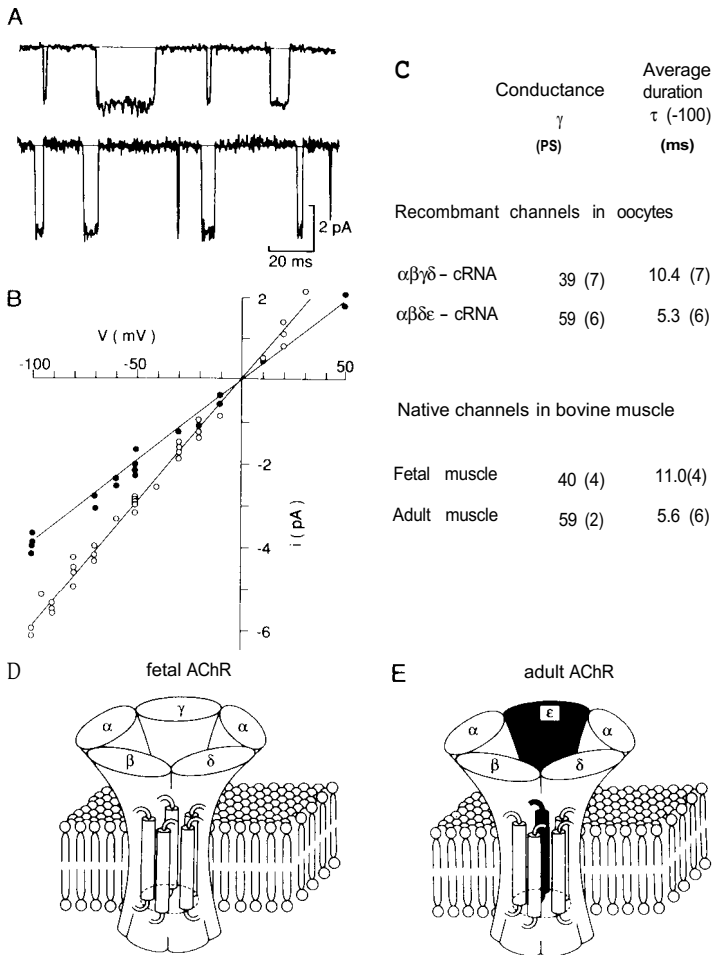


Figure 6. End-plate channel isoforms are specified by differences in subunit composition. A, B: Single channel currents and conductance mediated by recombinant AChR channels expressed in *Xenopus* oocytes previously injected with cRNAs encoding the subunit combinations α -, β -, γ - and δ - (upper trace and filled symbols) and α -, β -, δ and ϵ -subunits of bovine muscle AChR (lower trace and open symbols). C: Conductance and average open times of two isoforms of recombinant and native AChR channels from bovine skeletal muscle (modified from Mishina et al., 1986). D, E: Schematic diagram of the subunit composition of end-plate channel subtypes in fetal and adult skeletal muscle. The structure of the AChR is schematically drawn according to Unwin (1989).

from muscle at different postnatal ages show that a reciprocal change in the level of γ and ϵ -subunit specific mRNAs occurs during postnatal development (Witzemann et al., 1989; Witzemann et al., 1991). This differential regulation depends on differences in the regulatory sequences of the γ - and ϵ -subunit genes and their different responsiveness to neural and myogenic factors (Witzemann et al., 1990; Numberger et al., 1991; Witzemann and Sakmann, 1991). Since in most cells, including neurones, channel isoforms are expressed which often are colocalized in a mosaic-like manner, the

regulation of the abundance of channel isoforms by differential expression of subunit genes may be one mechanism by which long-term ('plastic') changes in chemical and electrical excitability can occur (Sakmann et al., 1992, for review).

Molecular determinants of ion transport: The work of Hille and coworkers (Hille, 1984) had indicated that the end-plate channel is a cation-selective pore with a channel constriction of about 6 Å in diameter. The first insight into the molecular determinants of ion transport of the AChR was obtained following the identification of sequence domains in each subunit that may participate in forming the wall of the channel. Conventional whole-cell current measurements from *Xenopus* oocytes, coinjected with wild type and mutagenized AChR subunit-specific cRNAs, gave only inconclusive results with respect to the involvement of particular subunit domains (Mishina et al., 1985). Subunit specific differences in gating and conductance of various channel isoforms were however detected by single channel conductance measurements from isolated membrane patches where the ion composition and concentration on both membrane faces could be varied (Hamill et al., 1981). These advantages were exploited to localize functionally important domains in AChR subunits.

Hybrid channels and chimaeric subunits: The gating and conductance of recombinant AChR channels assembled from homologous subunits of different species like *Torpedo californica* and calf (*bos taurus*) depends on the particular combination of subunit cRNAs coinjected (Sakmann et al., 1985). The δ -subunits of bovine muscle and of *Torpedo* electroplax AChR confer slightly different conductances to the hybrid channels when assembled together with α -, β - and γ -subunits of either species (Imoto et al., 1986). This observation was exploited to construct various chimaeric subunits from bovine and *Torpedo* AChR δ -subunits (Fig. 7A, R). Conductance measurements of the recombinant channels carrying different chimaeric δ -subunits (Fig. 7C) identified a domain designated as the M2 transmembrane segment to be important for conferring differences in conductance (Imoto et al., 1986). The most conspicuous difference in the aligned amino acid sequences was in the number of charged amino acids in the extracellular bend bordering the M2 segment (Fig. 7D).

The channels mouths and wall probed by conductance measurements of mutant channels: To precisely locate those amino acids important for ion transport and selectivity we investigated the effect of point mutations in the M2 transmembrane segment and the adjacent bends on conductances of mutant channels. Four amino acid positions, homologous in each subunit, were identified where amino acids are localized which are important for cation transport through the open channel and for its selectivity between monovalent cations.

Anionic rings: The M2 transmembrane regions, identified by mapping with chimaeric δ -subunits, show a conspicuous clustering of charged amino acids bordering the M2 transmembrane segment in each of the subunits (Fig. 8A). By introducing point mutations at these positions, which changed

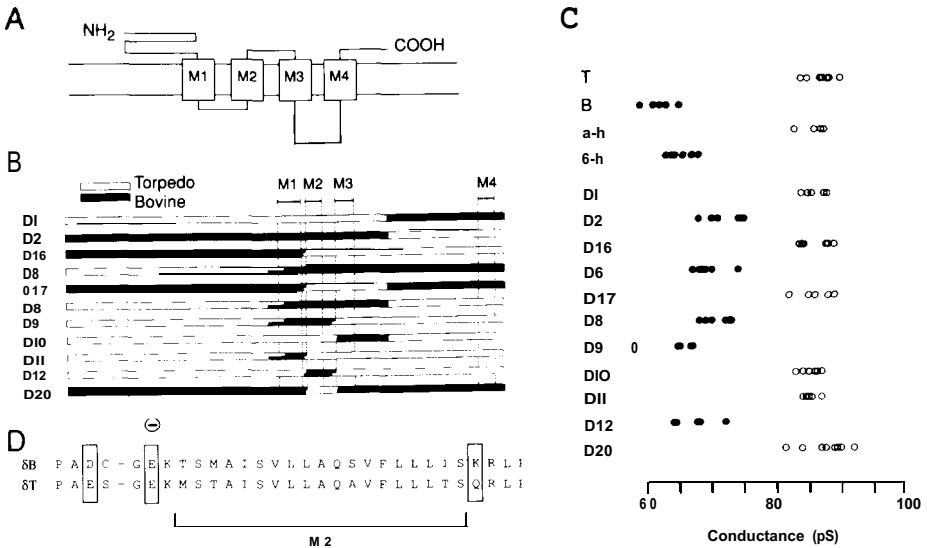


Figure 7. Localisation of M2 segment by single channel conductance measurements of recombinant AChR channels carrying different chimaeric δ -subunit constructs. A: Schematic drawing of assumed transmembrane folding of AChR subunits as suggested from hydropathy analysis. N- and C-terminal ends are extracellular. B: Chimaeric δ -subunit constructs derived from *Torpedo californica* electroplax and bovine skeletal muscle AChR α -subunits. C: Single channel conductance of recombinant AChR channels carrying chimaeric δ -subunits as shown in C. T and B refer to *Torpedo* or bovine muscle wild type channels respectively. D: Comparison of amino acid sequence of δ -subunits from bovine muscle and *Torpedo* electroplax AChR in their M2 transmembrane segment (single letter code). Note difference in charged amino acids in M2-M3 bend (modified from Imoto et al., 1986).

the charge of the amino acid side chains, we found that largely the net number of negative charges, irrespective in which subunit the mutation was introduced, determines the channel conductance. This suggested that the charged amino acids of the constituting subunits present in the bends bordering the M2 segment (Fig. 8A) are forming three ring-like structures at the channels extra- and intracellular mouths, respectively (Imoto et al., 1988; Konno et al., 1991).

Channel constriction: To localize positions where amino acid side chains are forming the channel wall and in particular those amino acids that form the narrow portion of the channel, we investigated the functional properties of recombinant AChR channels mutagenized within the M2 transmembrane segment. The narrow portion is often referred to as the channels 'selectivity filter' suggesting that here the interaction of transported ion, and their water shells, with the channels inner wall determines which ions may pass and which may not (Hille, 1984, for review). To map amino acids which could be involved in this interaction, conductances of mutant channels for different cations of different size and mobility were measured (Fig. 8B). These measurements indicated that a major determinant of ion selectivity resides in the residues located in M2 at a position close to the position

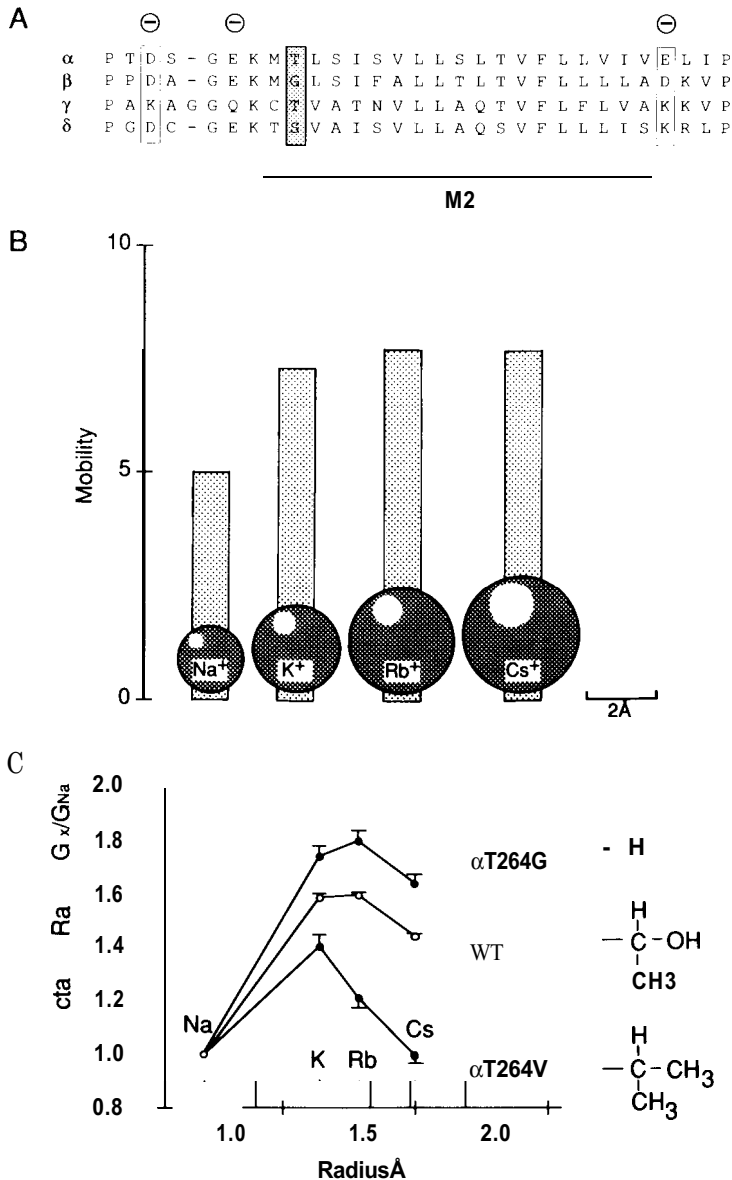


Figure 8. Localisation of selectivity filter of AChR channel by single channel conductance measurements of recombinant AChR channels carrying mutations in the M2 transmembrane segment. A: Sequence alignment of α -, β -, γ - and δ -subunits of rat muscle AChR in the M2 transmembrane segment and adjacent bends (single letter code). The location of clusters of charged amino acids forming anionic rings at the channels mouth's as identified in orpedo AChRs, are indicated by minus signs above the sequences. The amino acids forming the intermediate anionic ring are located in between those forming the intracellular ring (left) and the extracellular ring (right). The location of amino acids forming the constriction is indicated by the shaded box. B: Schematic representation of sizes and mobility of cations (modified from Atkins and Clugston, 1983) used to probe determinants of AChR channel conductance and selectivity. The scale on the left side represents ion mobility [in 10^{-4} (cm/s)/(V/cm)]. C: Conductance ratios of wild type (WT) and mutant channels carrying mutations in the cytoplasmic part of the α -subunit M2 segment (indicated by shaded box in A), where a threonine residue is replaced either by a valine (α T264V) or a glycine (α T264G) residue, for different size of cations (modified from Villarroel and Sakmann, 1992).

of amino acids forming the 'intermediate' anionic ring (Fig. 8A). The channel conductance is altered by introducing amino acids of different side chain volume at this position. Side chains like valine that have larger volumes reduce the conductance, while side chains with smaller volumes increase the conductance (Villarroel et al., 1991). The effect of these point mutations depends on the size and mobility of the ion used to measure the conductance (Fig. 8C), the effects being larger for Cs^+ than for Na^+ (Villarroel and Sakmann, 1992).

A simple model of the AChR selectivity filter: Single channel conductance measurements on hybrid AChR channels carrying chimaeric subunits thus identified the M2 transmembrane segment as one determinant contributing to the formation of the channels' inner wall. Point mutational analysis refined the mapping and identified four positions in each subunit where amino acid side chains are likely to interact with permeating cations. A working hypothesis would be to assume that cations accumulate at the channels' extra- and intracellular mouths because of electrostatic attraction via the negative charges provided by the three anionic rings, whereas anions are excluded because of electrostatic repulsion. The selection between monovalent cations is predominantly due to sieving in the channels constriction, which is formed by amino acids contributing hydroxyl-containing side chains.

ION CHANNELS MEDIATING RAPID SYNAPTIC TRANSMISSION BETWEEN NEURONES

Synapses in the central nervous system (CNS) operate using transmitters which are different from those in peripheral synapses, the most common ones being glycine, GABA, glutamate and serotonin. Moreover CNS-synapses fall into two categories, either excitatory or inhibitory. The work of Eccles and his collaborators (Eccles, 1963) showed that synaptic communication in the CNS, as in the periphery, is mediated by ionic currents that flow across the postsynaptic membrane, generating excitatory or inhibitory postsynaptic potentials (EPSPs and IPSPs). Depending on which ions carry the postsynaptic currents, the respective transmitters are classified as excitatory or inhibitory. Glutamate, serotonin and ACh activate cation currents, carried mostly by Na^+ and K^+ and to a smaller extent by Ca^{2+} under physiological conditions, whereas GABA and glycine activate anion currents, carried under physiological conditions by Cl^- . To characterize the elementary currents underlying postsynaptic potentials in the CNS we initially used isolated neurones obtained from fetal brain, maintained in culture conditions, which express receptor channels activated by CNS transmitters.

Elementary currents activated by glycine and GABA: An important feature of signal integration in the CNS is the occurrence of postsynaptic inhibition between neurones. This occurs when the electrical activity of a neurone is reduced by IPSPs, which are largely mediated by the transmitters glycine or

GABA, which cause an increase in the permeability of the postsynaptic cell to chloride ions. To find out whether ion channels mediate this increase in Cl^- conductance we measured the elementary currents activated by glycine or GABA in neurones isolated from fetal spinal cord and brain. They were freed from their extracellular coats during the isolation procedure and readily allow the sealing of a pipette tip onto their plasma membrane (Fig. 9A).

For the characterisation of the ionic requirements of currents and pharmacology activated by inhibitory transmitters the 'whole-cell' recording configuration (Fig. 9B) was used, thus allowing the current through the entire cell membrane to be monitored. Fig. 9C illustrates the activation of membrane current of hundreds of pA in a spinal neurone in response to the application of glycine. The current trace becomes "noisy" during glycine activated current, but elementary currents are not resolvable. Following isolation of an 'outside-out' patch (Fig. 9D) the application of glycine at the same concentration activates a much smaller average current, of only a few pA. The superposition of pulse-shaped elementary currents is now clearly detectable (Fig. 9E), suggesting that glycine activated whole-cell currents are generated by the superposition of elementary currents of unitary amplitude and varying duration. The size of glycine-activated elementary currents is in the same range as that of elementary end-plate currents, indicating that CNS transmitters also act by opening ion channels.

Coactivation of GlyR and GABAR channels: Most neurones isolated from fetal CNS have both glycine and GABA activated whole-cell currents which are carried by Cl^- . The respective ion channels (GlyR- and GABAR-channels) were often co-localized in the same membrane patch (Fig. 10A) and their properties were studied by recording single channel currents.

The GlyR and GABAR-channels are different molecular entities (Betz, 1990) which share many functional properties. By measuring the reversal potentials in bi-ionic conditions using different permeant inorganic and organic anions the diameter of the narrow region of GlyR and GABAR channels was found to be between 4.8 and 5.4 Å at its constriction (Bormann et al., 1987). This is comparable to the size of the constriction of the end-plate channel (Hille 1984, for review). The results suggest, in conjunction with structural information obtained from the elucidation of the amino acid sequences of the constituting GlyR and GABAR subunits, that transmitter gated channels are operating according to common principles, possibly being derived from common evolutionary ancestors (Betz, 1990, for review).

Conductance substates of channels activated by CNS transmitters: The elementary currents activated by glycine or GABA are pulse shaped events, but in contrast to what we had expected initially, both transmitters opened channels which may adopt several conductance states. Several of these substates are common to both channels, however the most frequently occurring "main" conductance states are different (Hamill et al., 1983; Bormann et al., 1987). Glutamate, the major excitatory transmitter in the CNS, also

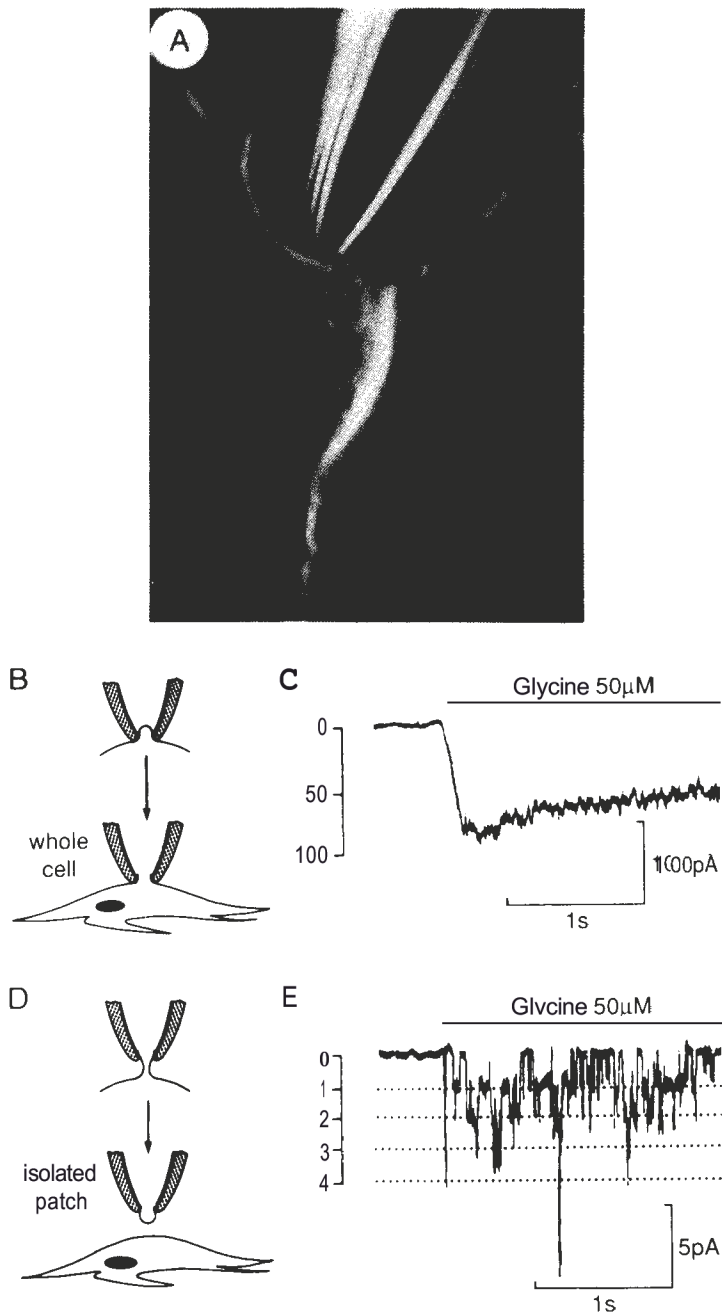


Figure 9. Noisy whole-cell and pulse shaped elementary currents activated by glycine in isolated neurone maintained in tissue culture. A: Photomicrograph of cell body of a cultured neurone and tip of patch pipette touching cell membrane. Calibration bar is $10\ \mu\text{m}$. B: Schematic diagram of recording configuration to measure whole-cell current from isolated neurone. C: Record of whole-cell current in response to application of inhibitory transmitter glycine. Note noisy trace during glycine activated current. Scale on the left refers to number of open channels. D: Schematic diagram of recording configuration to measure elementary currents from outside-out patch, isolated from neuronal cell body. E: Record of elementary currents in response to glycine application to outside-out membrane patch. Scale refers to number of open channels (modified from Sakmann et al., 1983).

activates elementary currents in the range of pA which fall into several amplitude classes, indicating that glutamate receptor (GluR) channels also adopt substates (Ascher and Nowak, 1988; Cull-Candy and Usowicz, 1987; Jahr and Stevens, 1987). So far, the mechanism and the possible functional significance of conductance substates remain poorly understood. The analy-

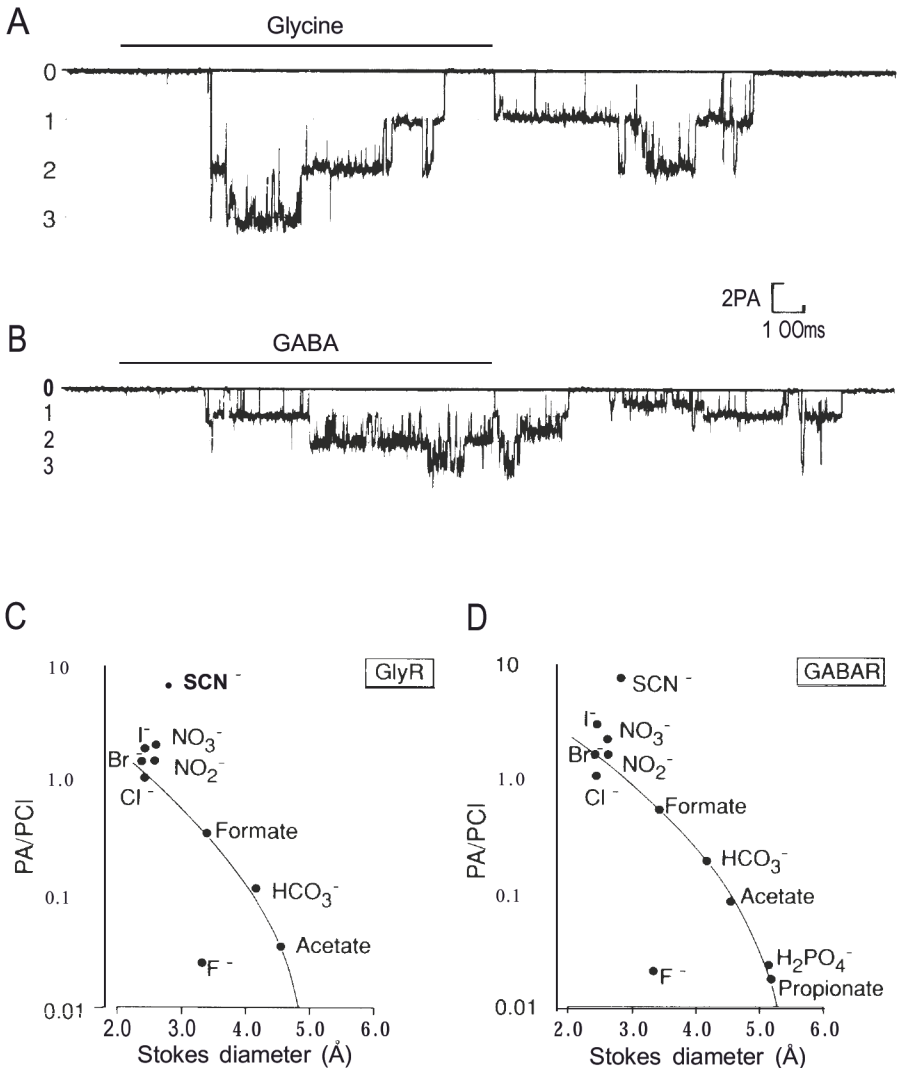


Figure 10. Coactivation of GlyR and GABAR-channels. A: Single channel currents activated by glycine in an outside-out patch from a mouse spinal neurone. Several GlyR channels are activated in this patch, as indicated by scale on left side, and elementary GlyR channel currents are superimposed. B: Single channel currents activated by gamma-aminobutyric acid (GABA) in the same patch as shown in A. Superposition of elementary currents indicates the presence of several GABAR channels in this patch. C, D: Size of narrow part of GlyR and GABAR channels, mapped by reversal potential measurements in biionic conditions with chloride versus with organic anions of different size. Extrapolated diameters of constriction of GlyR and GABAR channels are very similar, between 4.8 and 5.4 Å (from Bormann et al., 1987).

sis of recombinant channels indicate that the receptor channels gated by the major CNS transmitters, GABA, glycine and glutamate can show a wide functional diversity. This probably occurs due to the expression of numerous subunits, which may form both homo- as well as heterooligomeric isoforms of channels with subunit-specific properties (Verdoorn et al., 1990). A possible, but so far unproven hypothesis would be that channel subtypes are co-localized in the postsynaptic membrane in a mosaic-like fashion; this may be a prerequisite for the alteration of synaptic efficacy by changes in the composition of isoforms of the receptor mosaic.

POSTSYNAPTIC CURRENTS IN BRAIN SLICES

It is important to characterize those receptor channel isoforms that actually mediate postsynaptic potentials in neurones of clearly defined pathways in the intact CNS. In culture the cellular identity of isolated neurones is rather ill-defined, and these neurones lack their natural neighbours with which they form specific synapses. Therefore, the brain slice technique, pioneered by P. Andersen, was modified to perform whole-cell and single channel current measurements from neurones in situ, to characterize the quantal conductance changes generating EPSPs and IPSPs and the elementary currents underlying them.

Sealing patch pipettes, onto new-ones in brain slices: The procedure that allowed us to use patch pipettes for whole-cell and single channel conductance measurements on neurones in brain slices consisted of a modification of the procedure developed for exposing the end-plates of single skeletal muscle fibres. Initially we used local application of collagenase; however, we found later that a gentle stream of extracellular solution, directed towards the surface of the slice (Fig. 11 A), was sufficient to expose the cell body of visually identified neurones (Fig. 11 B, C) in almost any part of the brain or spinal cord for recording with patch pipettes (Edwards et al., 1989).

Quantal transmission in CNS synapses: Recording of stimulus-evoked IPSCs from granule cells of the dentate gyrus, as well as recording of elementary currents from outside-out patches, demonstrated the quantal nature of IPSCs mediated by GABA, and showed that the size of the conductance change occurring during a quantal IPSCs is relatively small (in the order of 100 – 200 pS). This suggested that only a small number of postsynaptic GABAR channels (20 to 40) are activated by the release of a quantum of transmitter. Based on results from modelling the size and time course of IPSCs it appears that the small number of activatable GABAR-channels under a single synaptic bouton is the major determinant of this small quantal conductance change (Sakmann et al., 1989; Edwards et al., 1990; Busch and Sakmann, 1991).

Recording of stimulus evoked EPSCs from neurones where synaptic knobs are located at or close to the cell body, such as in stellate cells in layer IV of visual cortex (Fig. 12A) or from pyramidal cells of the hippocampal CA3 region where mossy fibre terminals form synapses on the shaft of the

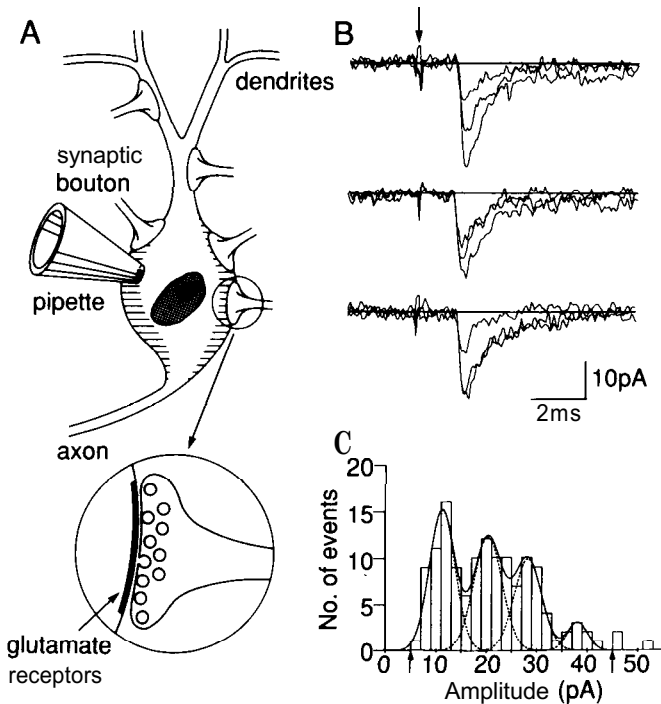


Figure 12. Excitatory postsynaptic currents in CNS neurone mediated by glutamate acting on glutamate receptors. A: Schematic diagram of whole-cell recording of excitatory postsynaptic currents (EPSCs) from a neurone in a brain slice where glutamate is released from vesicles to act on postsynaptic glutamate receptors (GluR). B: Examples of stimulus evoked EPSCs mediated by glutamate acting on GluR channels of the AMPA/KA subtype. Time of electrical stimulus delivered to a neighbouring neurone is indicated by arrow. Three responses are superimposed in each set of traces to illustrate the fluctuation in peak amplitude of EPSCs in response to a constant stimulus. Three uppermost traces correspond to one, two and three quantal events, respectively. C: Amplitude distribution of stimulus evoked EPSCs. Peaks in this distribution indicate that EPSCs are quantal in nature with a quantal conductance change on the order of 100 pS (from Stern et al., 1992).

apical dendrite, also demonstrated the quantal nature of EPSCs mediated by glutamate acting on postsynaptic glutamate receptor (GluR) channels of the AMPA subtype (Jonas and Sakmann, 1992; Stern et al., 1992). EPSCs are also characterized by a small quantal conductance change, in the order of 100 – 200 pS (Fig. 12B), which most likely also reflects a small number of activated channels.

Gating of GluR channels in CNS synapses: In central synapses the time course of the changes in transmitter concentration following axonal release is not known, nor is the density or the kinetic properties of the receptor channels. If the transmitter disappears rapidly from the synaptic cleft, the decay of EPSCs or IPSCs would reflect the distribution of elementary current durations after removal of the transmitter. Alternatively, the decay could reflect desensitization of postsynaptic receptors in the presence of a sustained level of transmitter in the synaptic cleft. To measure the gating

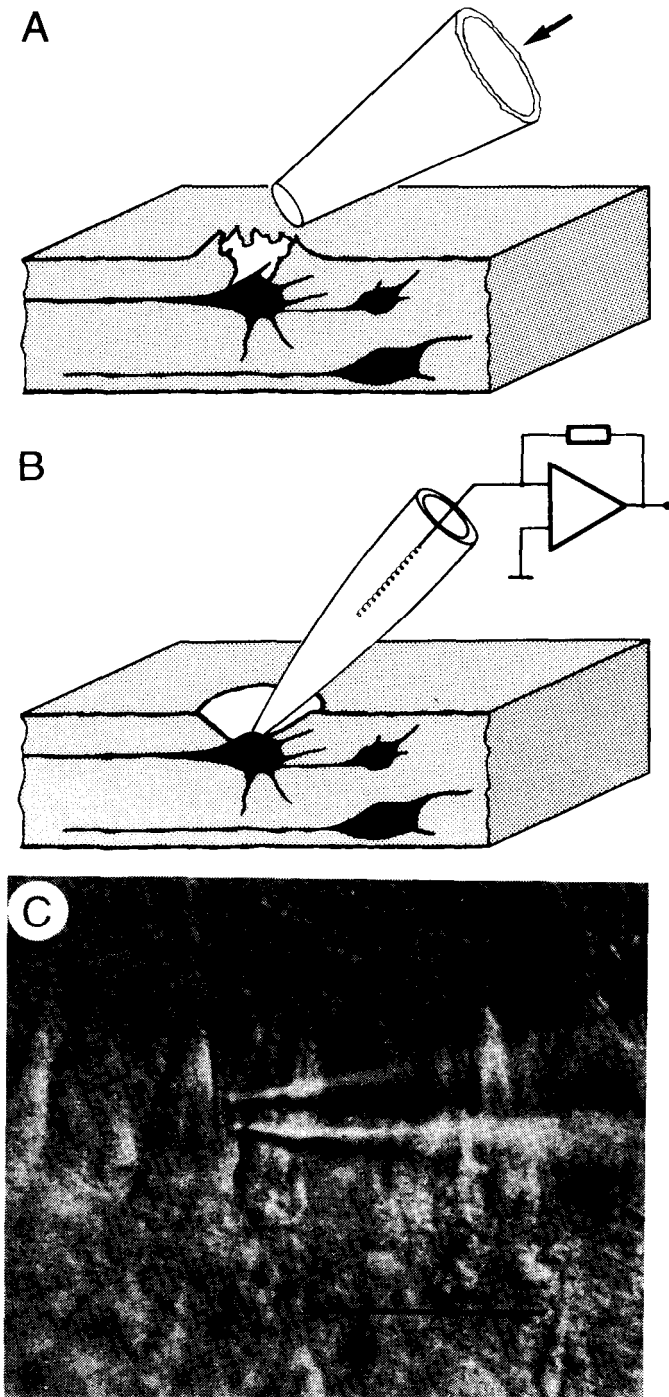


Figure 11. Exposure of CNS neurones in brain slices for current recording with patch pipettes. A: Schematic drawing of the procedure used to expose the soma of individual neurones in brain slices. The tissue covering the cell body is removed by a gentle stream of extracellular solution delivered from a small pipette. B: Tip of patch pipette is sealed onto exposed cell body. C: Photomicrograph of exposed soma of hippocampal pyramidal neurone in rat brain slice. The tip of pipette used to deliver a stream of extracellular solution is visible on the right side. Calibration bar is 20 μm . (Modified from Edwards et al., 1989).

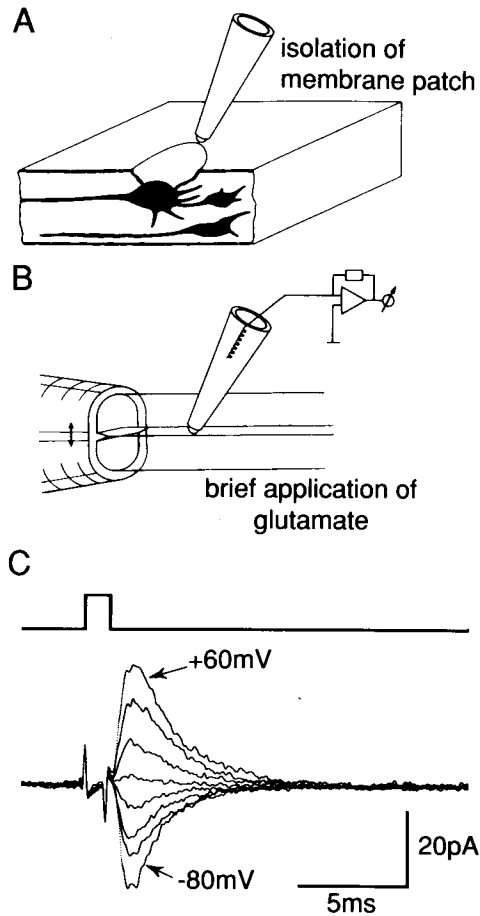


Figure 13. Characterisation of native GluR-channels in CNS neurone of a brain slice. **A:** Schematic diagram of isolation of outside-out patch from the soma of a neurone in a brain slice. **B:** Schematic diagram of method of brief agonist application to an outside-out patch. The tip of the patch pipette, sealed by the outside-out patch, is brought close to the opening of a double barrelled application pipette delivering two solution streams, one with control solution, the other containing in addition 1 mM L-glutamate. The pipette is moved briefly by 10–20 μm by means of a Piezo-element to expose patch to a pulse of glutamate. **C:** Family of currents in response to glutamate application to membrane patch isolated from a rat hippocampal cell at different membrane potentials (at 20 mV intervals). Duration of glutamate application is 1 ms as indicated in upper trace. Current rises rapidly (less than 1 ms) to peak. Decay time constants of current following removal of glutamate is 2–3 ms. Modified from Colquhoun et al.(1992)

properties of postsynaptic receptor channels in the CNS we used a method that allows brief agonist applications to outside-out membrane patches (Franke et al., 1987), isolated from neurones in an anatomically clearly-defined region of the brain (Fig. 13A, B).

The experiments showed that although closure of GluR channels by desensitization is fast, it is considerably slower than closure of channels to the resting state following removal of agonist (Fig. 13C) (Colquhoun et al., 1992). It is, in particular, slower than the decay of EPSCs, for example from

excitatory synapses on stellate cells (Stern et al., 1992), suggesting that, at least in these cells, the decay of the fast EPSCs reflects predominantly the closure of GluR channels from the open to the resting closed state following rapid removal of transmitter from the synaptic cleft. This implies that glutamate is present only very briefly in the synaptic cleft (less than 1 ms) and that EPSCs are mediated by a GluR channel subtype characterized by short average duration of elementary currents. In spite of this some desensitisation of GluR channels may still occur, even during a single EPSC (Trussell and Fischbach, 1989).

Molecular determinants of GluR-channel function: To find out whether the occurrence of functional GluR channel subtypes which mediate rapid synaptic currents is based on the assembly of native channels from different subunit combinations, which may confer different properties to the assem-

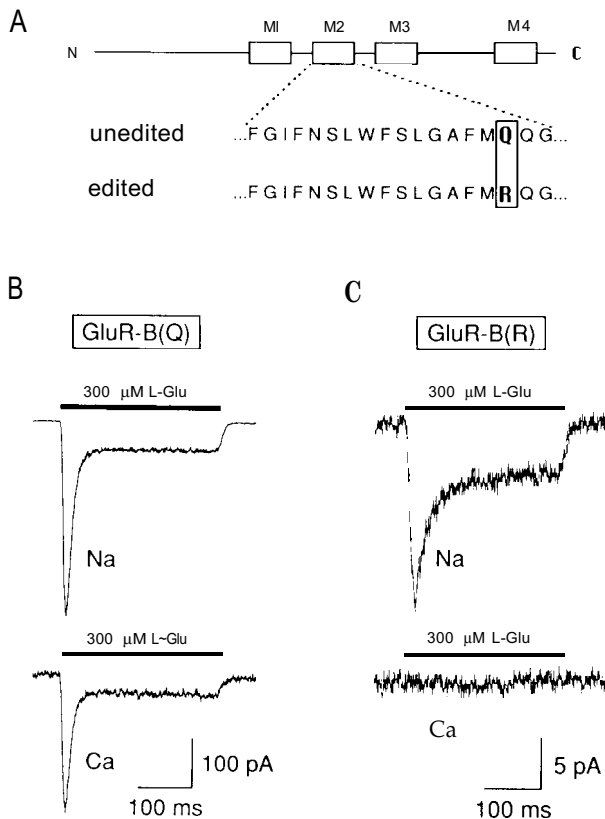


Figure 14. Characterisation of recombinant GluR-channel subtypes expressed in host cell. A: Differences in amino acid sequence of GluR-channel subunits in M2 transmembrane segment of GluR-B subunit. Box indicates amino acid present at Q/R site in two isoforms of this subunit, GluR-B(Q) and CluR-B(R). The presence of arginine at this site is the consequence of mRNA editing. B: Functional properties of recombinant GluR-channels assembled from unedited GluR-B(Q) subunits. Inward current activated by glutamate is carried both by Na and Ca. C: Functional properties of recombinant CluR channels assembled from edited GluR-B(R) subunits. In the presence of high extracellular Na an inward current is activated whereas with high extracellular Ca no inward current is observed (modified from Burnashev et al., 1992).

bly, we collaborated with P. Seeburg and compared functional properties of native and recombinant GluR channels. Recombinant GluR channels were assembled from different subunits of the AMPA receptor subunit family (Hollmann et al., 1989; Keinänen et al., 1990) guided by the pattern of subunit genes which are co-expressed in different parts of the brain (Sommer et al., 1990).

Comparison of functional properties of recombinant homomeric and heteromeric GluR channels suggested that properties like rectification of channel conductance and divalent permeability are dominated by the presence of a particular (GluR-B) subunit in native GluR channels (Hollmann et al., 1991; Verdoorn et al., 1991). This dominance was traced to a single amino acid in the putative M2 transmembrane segment (Verdoorn et al., 1991; Hume et al., 1991; Bumashv et al., 1992). The almost ubiquitous expression of the GluR-B subunit gene in CNS is likely to confer the conductance properties and the low Ca^{++} permeability of native GluR channels mediating fast EPSCs. Its differential expression is likely to determine differences in Ca^{++} permeability of native GluR channels in different cell types, for example of the cerebellum (Khodorova and Burnashev, 1992). In addition to differential expression of the GluR-B subunit gene an additional mechanism seems to operate in regulating the properties of native GluR channel isoforms. The GluR-B subunit is found in two isoforms differing only by a single amino acid in the M2 transmembrane segment (Fig. 14A-C). The two subunit isoforms confer different conductance properties to heteromeric channels. The difference is most likely due to editing of the GluR-B subunit specific mRNA (Sommer et al., 1991).

OUTLOOK

Patch clamp techniques are now well established and routinely applied in combination with other techniques like recombinant DNA or fluorimetric techniques to characterize molecular details of the events underlying synaptic signalling between cells. Through the measurement of elementary currents the biophysical interpretation of the electrical signals which underlie rapid cellular communication across synapses has been simplified and can be partly understood in molecular terms. At the same time single channel conductance measurements have provided evidence for numerous isoforms of receptor channels, as well as voltage and second messenger gated channels particularly in CNS neurones. The significance of this remains to be elucidated with respect to synaptic communication in the CNS. It seems that the characterisation of the various types of ligand and voltage gated ion channels on the extensive dendritic trees of CNS neurones is necessary for an understanding of their integrative function, i. e. the generation of patterns of electrical activity resulting from IPSPs and EPSPs from many synaptic inputs. Equally important will be the characterisation of the ion channels responsible for the electrical activity of nerve terminals. Patch pipettes could provide the resolution necessary to study the electrical

signals in nerve terminals and dendrites. This seems to be a prerequisite if one wishes to understand how changes in synaptic transmission may contribute to changes in functional connectivity of neuronal pathways, during normal and pathological states.

ACKNOWLEDGEMENTS

I am greatly indebted to my teachers in physiology, Otto Creutzfeldt and Bernard Katz, and to the Max-Planck-Gesellschaft for providing ideal research conditions. During the last five years I was supported by the Leibniz Program of the Deutsche Forschungsgemeinschaft and by an award of the Foundation Louis Jeantet, Geneva.

REFERENCES

- Anderson, C. R. and C. F. Stevens, *J. Physiol.* 235, 655 (1973).
 Ascher, P., and L. Nowak, *J. Physiol.* 399, 227 (1988).
 Atkins, P. W. and M. J. Clugston, *Principles of Physical Chemistry*. Pitman Publishing Limited, London, 1983.
 Axelson, J. and S. Thesleff, *J. Physiol.*, 147, 178 (1959).
 Betz, H., *Biochemistry*, 29, 3591 (1990).
 Betz, W. and B. Sakmann, *J. Physiol.*, 230, 673 (1973).
 Bormann, J., O. P. Hamill and B. Sakmann, *J. Physiol.*, 385, 243 (1987).
 Burnashev, N., H. Monyer, P. H. Seeburg and B. Sakmann, *Neuron*, 8, 189, (1992).
 Busch, C., and B. Sakmann, in: The Brain. Cold Spring Harbor Symp. *Quant. Biol.* Vol. LV. Cold Spring Harbor Laboratory Press, pp. 69-80 (1990).
 Colquhoun, D. and A. G. Hawkes, *Proc. Roy. Soc. B* 199, 231 (1977).
 Colquhoun, D. and A. G. Hawkes, *Phil. Trans. Roy. Soc. B* 300, 1 (1982).
 Colquhoun, D. and B. Sakmann, *Nature*, 294, 464 (1981).
 Colquhoun, D. and B. Sakmann, *J. Physiol.*, 369, 501 (1985).
 Colquhoun, D., P. Jonas and B. Sakmann, *J. Physiol.*, 1992 (in press).
 Cull-Candy, S. G., and M. M. Usowicz, *Nature*, 325, 525 (1987).
 Del Castillo, J. and B. Katz, *Proc. Roy. Soc. B* 146, 369 (1957).
 Eccles, J. C., in: *Les Prix Nobel en 1963*, pp. 261-283, Stockholm: The Nobel Foundation.
 Edwards, F. A., A. Konnerth, B. Sakmann and T. Takahashi, *Pflügers Arch.*, 414, 600 (1989).
 Edwards, F. A., A. Konnerth, B. Sakmann, with an appendix by C. Busch, *J. Physiol.*, 430, 213 (1990).
 Franke, C., H. Hatt and J. Dudel, *Neuroscience Lett.* 77, 199 (1987).
 Hamill, O. P., J. Bormann and B. Sakmann, *Nature*, 305, 805 (1983).
 Hamill, O. P., A. Marty, E. Neher, B. Sakmann and F. Sigworth, *Pflügers Arch.*, 391, 85 (1981).
 Hamill, O. P. and B. Sakmann, *Nature*, 294, 462 (1981).
 Hille, B., *Ionic Channels of Excitable Membranes* (Sinauer Associates Inc. Sunderland, Massachusetts) (1984).
 Hollmann, M., A. O'Shear-Greenfield, W. Rogers and S. Heinemann, *Nature*, 342, 643 (1989).
 Hollmann, M., M. Hartley and S. Heinemann, *Science*, 252, 851 (1991).
 Hume, R. I., R. Dingledine and S. Heinemann, *Science*, 253, 1028 (1991).
 Imoto, K., C. Methfessel, B. Sakmann, M. Mishina, Y. Mori, T. Konno, K. Fukuda, M. Kurasaki, H. Bujo, Y. Fujita and S. Numa, *Nature*, 324, 670 (1986).

- Imoto, K., C. Busch, B. Sakmann, M. Mishina, T. Konno, J. Nakai, H. Bujo, Y. Mori, K. Fukuda and S. Numa, *Nature*, **335**, 645 (1988).
- Jahr, C. E., and C. F. Stevens, *Nature*, **325**, 522 (1987).
- Jonas, P. and B. Sakmann, *J. Physiol.*, (1992) (in press).
- Karlin, A., *The Harvey Lecture Series* **85**, 121 (1991).
- Katz, B., *Nerve, Muscle and Synapse*. McGraw Hill Book Co., New York (1966).
- Katz, B., *The Release of Neural Transmitter Substances*, The Sherrington Lectures X, Liverpool University Press, (1969).
- Katz, B. and R. Miledi, *J. Physiol.* **224**, 665 (1972).
- Keinanen, K., W. Wisden, B. Sommer, P. Werner, A. Herb, T. A. Verdoorn, B. Sakmann and P. H. Seeburg, *Science*, **249**, 556 (1990).
- Khodorova, A., and N. Burnashev, *J. Physiol.*, **446**, 516 P (1992).
- Konno, T., C. Busch, E. von Kitzing, K. Imoto, F. Wang, J. Nakai, M. Mishina, S. Numa and B. Sakmann, *Proc. R. Soc. Lond., B* **244**, 69 (1991).
- Magleby, K. L. and C. F. Stevens, *J. Physiol.* **223**, 173 (1972).
- Methfessel, C., V. Witzemann, T. Takahashi, M. Mishina, S. Numa and B. Sakmann, *Pflügers Arch.* **407**, 577 (1986).
- Michler, A., and B. Sakmann, *Dev. Biol.*, **80**, 125 (1980).
- Miledi, R., I. Parker and K. Sumikawa, in: *Fidia Research Foundation Neuroscience Award Lectures, vol. 3*. New York: Raven Press, pp. 57-90, (1989).
- Mishina, M., T. Tobimatsu, K. Imoto et al., *Nature*, **313**, 364 (1985).
- Mishina, M., T. Takai, K. Imoto, M. Noda, T. Takahashi, S. Numa, C. Methfessel and B. Sakmann, *Nature*, **321**, 406 (1986).
- Neher, E., in: *Les Prix Nobel en 1991*, Stockholm: The Nobel Foundation.
- Neher, E. and B. Sakmann, *J. Physiol.*, **253**, 705 (1976a).
- Neher, E. and B. Sakmann, *Nature*, **260**, 799 (1976b).
- Neher, E., B. Sakmann and J. H. Steinbach, *Pflügers Arch.*, **375**, 219 (1978).
- Numa, S., *The Harvey Lecture Series*. **83**, 121 (1989).
- Numberger, M., I. Durr, W. Kues, M. Koenen and V. Witzemann, *EMBO J.*, **10**, 2957 (1991).
- Sakmann, B., *Fed. Proc.*, **37**, 2654 (1978).
- Sakmann, B. and H. R. Brenner, *Nature*, **276**, 401 (1978).
- Sakmann, B., J. Patlak and E. Neher, *Nature*, **286**, 71 (1980).
- Sakmann, B., O. P. Hamill and J. Bormann, *J. Neural Transm., Suppl.* **18**, 83 (1983).
- Sakmann, B., C. Methfessel, M. Mishina, T. Takahashi, T. Takai, M. Kurasaki, K. Fukuda and S. Numa, *Nature*, **318**, 539 (1985).
- Sakmann, B., F. Edwards, A. Konnerth and T. Takahashi, *Q. J. Exptl. Physiol.* **74**, 1107 (1989).
- Sakmann, B., V. Witzemann and H. Brenner, in: *Fidia Research Foundation Neuroscience Award Lectures, Vol 6.*, New York, Raven Press, pp. 53 – 103 (1992).
- Sommer, B., K. Keinanen, T. A. Verdoorn, W. Wisden, N. Burnashev, A. Herb, M. Köhler, T. Takagi, B. Sakmann and P. H. Seeburg, *Science*, **249**, 1580 (1990).
- Sommer, B., M. Köhler, R. Sprengel and P. H. Seeburg, *Cell*, **67**, 11 (1991).
- Stern, P., F. A. Edwards and B. Sakmann, *J. Physiol.* **449**, 247 (1992).
- Trussell, L. O. and G. D. Fischbach, *Neuron*, **3**, 209 (1989).
- Unwin, N., *Neuron*, **3**, 665 (1989).
- Verdoorn, T. A., A. Draguhn, S. Ymer, P. H. Seeburg and B. Sakmann, *Neuron*, **4**, 919 (1990).
- Verdoorn, T. A., N. Burnashev, H. Monyer, P. H. Seeburg and B. Sakmann, *Science*, **252**, 1715 (1991).
- Villarroel, A., S. Herlitze, M. Koenen and B. Sakmann, *Proc. Roy. Soc. Lond. B*, **243**, 69 (1991).
- Villarroel, A., and B. Sakmann, *Biophys. J.*, **62** 196 (1992).
- Witzemann, V., B. Barg, Y. Nishikawa, B. Sakmann and S. Numa, *FEBS Lett.*, **223**, 104 (1987).

- Witzemann, V., B. Barg, M. Criado, E. Stein and B. Sakmann, *FEBS Lett.* 242, 419 (1989).
- Witzemann, V., E. Stein, B., Barg, T. Konno, M. Koenen, W. Kues, M. Criado, M. Hofmann and B. Sakmann, *Eur. J. Biochem.*, 194, 437 (1990).
- Witzemann, V., H. R. Brenner and B. Sakmann, *J. Cell Biol.*, 114, 125 (1991).
- Witzemann, V., and B. Sakmann, *FEBS* 282, 259 (1991).